CO₂ capture by anion-functionalized deep eutectic solvents: the effect of steric hindrance of –OH groups

Mingzhe Chen,[a, #] Shaoyu Zhang,[b, #] Qingqing Mei,[b, *] Huacong Zhou, [c,*] and Dezhong Yang[a, *]

[a]School of Science, China University of Geosciences, Beijing 100083, China

[b]Institute of Environment Science and Technology, College of Environmental and Resource Sciences, Zhejiang University, Hangzhou 310058, Zhejiang, China

[c]College of Chemical Engineering, Inner Mongolia University of Technology; Inner Mongolia Key Laboratory of Green Chemical Engineering; Key Laboratory of CO₂ Resource Utilization at Universities of Inner Mongolia Autonomous Region, Hohhot, 010051, China.

[#] These authors contributed equally to this work.

Experimental Sections

Materials and Characterization

Ethylene glycol (99.5%) and pinacol (99 %) were purchased from J&K Scientific (Beijing). 1,2,3-triazole (98 %) was purchased from Innochem (Beijing). N,N-diethyl-N-methyl-N-(2-methoxyethyl)ammonium bromide ([MOEN$_{221}$][Br], 99 %) was purchased from Lanzhou Green Chemistry Co. Ltd., China. CO_2 (99.995%) and N_2 (≥99.99 %) were obtained from Beijing ZG Special Gases Science Co. Ltd. (Beijing, China). Ambersep 900(OH) ion exchange resin was supplied by Alfa Aesar. FTIR spectra were collected on a Nicolet 6700 spectrometer with an attenuated total reflection (ATR) accessory. ^{1}H NMR (400 MHz) and ^{13}C NMR (100.6 MHz) spectra were recorded on a Bruker spectrometer with DMSO-d_6 as the internal or external reference. EG was dried at room temperature by 4Å molecular sieve, and PIN was dried at 50 °C by 4Å molecular sieve prior to use. The water contents of the absorbents used in this work were determined using a Karl-Fischer titrator. The water contents of all absorbents (IL or DESs) were less than 700 ppm.

Synthesis of ILs and DESs

Synthesis of [MOEN$_{221}$][Tz]: at first, the mixture of Ambersep 900(OH) ion exchange resin and water was added to a glass column. The aqueous solution of [MOEN$_{221}$][Br] was then transformed to [MOEN$_{221}$][OH] solution after flowing through the column containing the resin. The concentration of [MOEN$_{221}$][OH] solution was titrated by potassium hydrogen phthalate. After that, equimolar 1,2,3-triazole was added into the solution of [MOEN$_{221}$][OH] ([MOEN$_{221}$][OH]: 1,2,3-triazole = 1 : 1). The mixture was stirred for about 2 h at room temperature. Then, water in the solution was removed using a rotary evaporator to obtain the liquid IL [MOEN$_{221}$][Tz], which was dried under vacuum at 70 °C prior to use.

Synthesis of DESs: [MOEN$_{221}$][Tz] was mixed with the alcohols (EG or PIN) at desired molar ratios at room temperature to obtain binary DESs used in this work. For ternary DESs, the three components [MOEN$_{221}$][Tz], EG, and PIN were mixed at desired molar ratios at room temperature.

Absorption and desorption of CO_2

The absorption and desorption procedures can be found in our previous work. [1-2] Briefly, CO_2 was bubbled into the absorbents contained in a glass tube during CO_2 absorption process, the capacity

of absorbents can be determined by the weight change of the glass tube. For CO_2 desorption, N_2 was bubbled into the solutions after absorption to release CO_2.

Computational methodology

All calculations were carried out using the Gaussian 16 software package [3] with the M06-2X/Def2TZVP method.[4,5] The temperature was set to 298.15 K. A custom implicit solvent model (SMD) [6] is used to describe the polar part of the solvent effect in the environment of each structure. Geometries of all structures were optimized at the aforementioned level of theory. Frequency analyses were also performed at the same level to confirm that the optimized geometries were free of imaginary frequencies. Gibbs free energies and distance between specific atoms of the computational systems were evaluated.
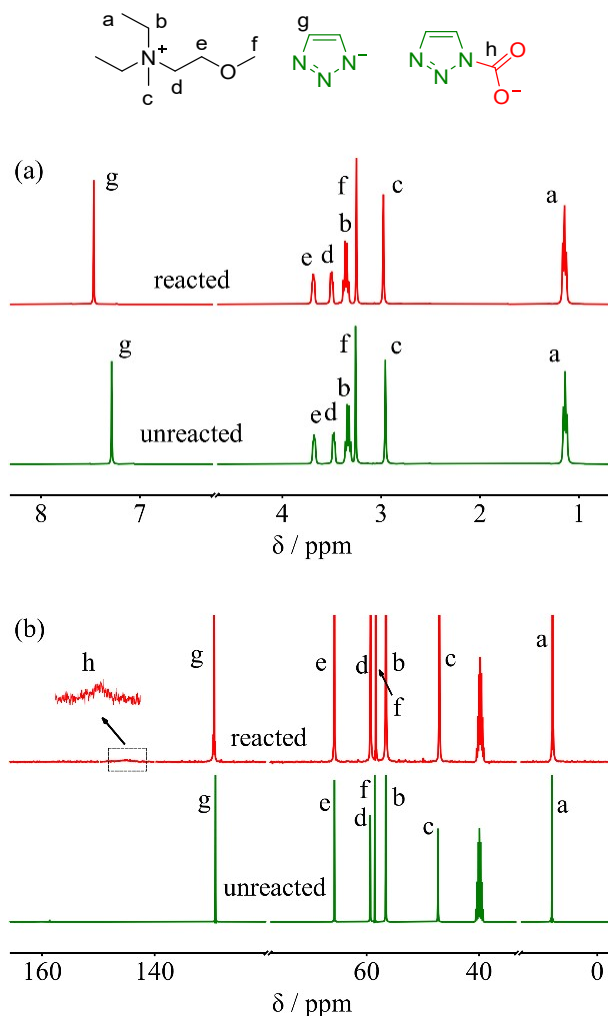
Fig. S1 The ^1H (a) and ^{13}C (b) NMR spectra of [MOEN$_{221}$][Tz] before and after CO_2 uptake.
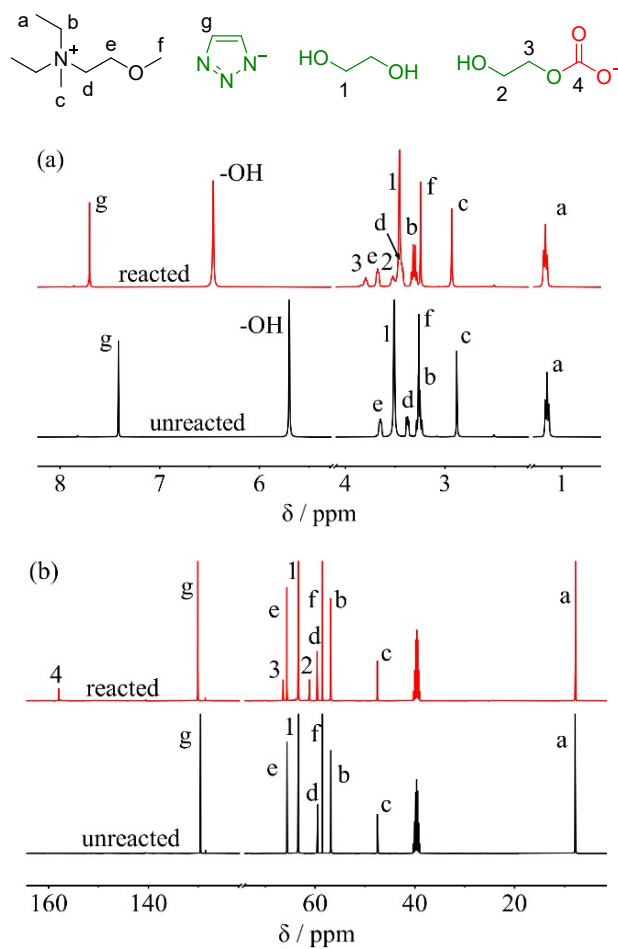
Fig. S2 The ^1H (a) and ^{13}C (b) NMR spectra of [MOEN$_{221}$][Tz]:EG (1:3) before and after CO_2 uptake.
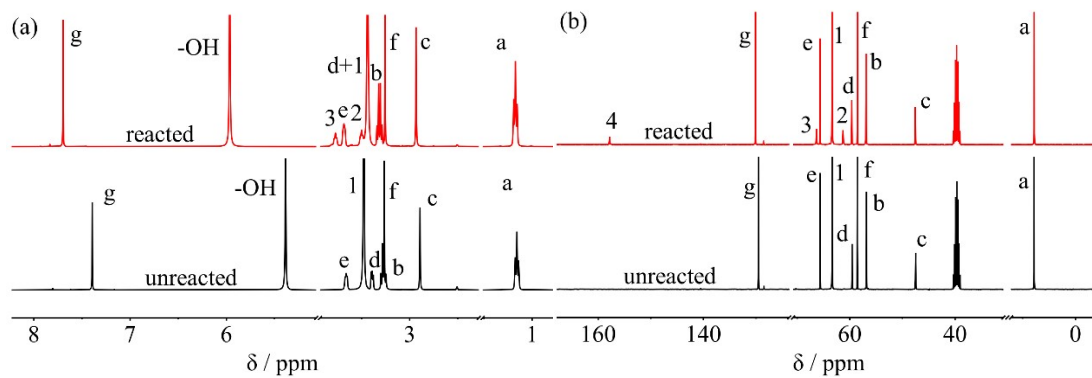
Fig. S3 The ^1H (a) and ^{13}C (b) NMR spectra of [MOEN$_{221}$][Tz]:EG (1:4) before and after CO_2 uptake.

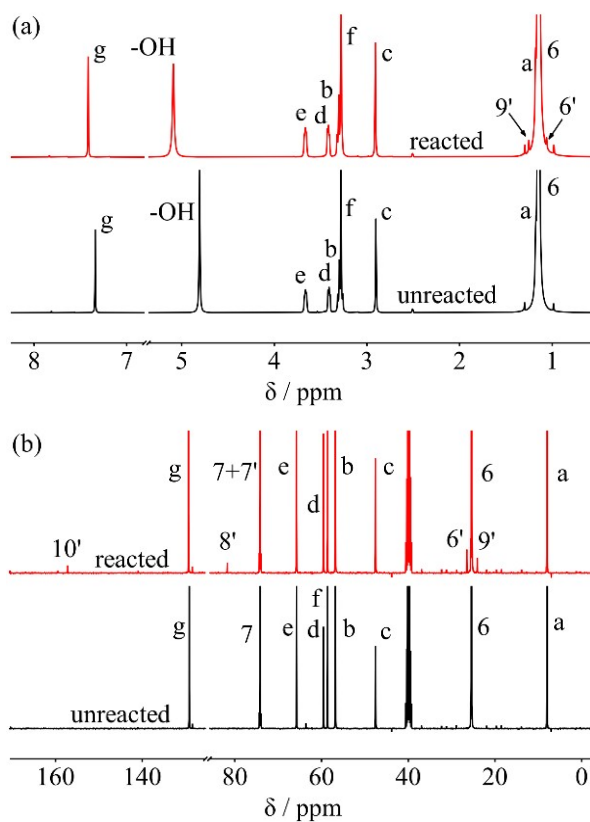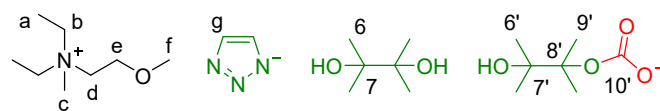**Fig. S4** The ^1H (a) and ^{13}C (b) NMR spectra of $[MOEN_{221}][Tz]$:PIN (1:3) before and after CO_2 uptake.
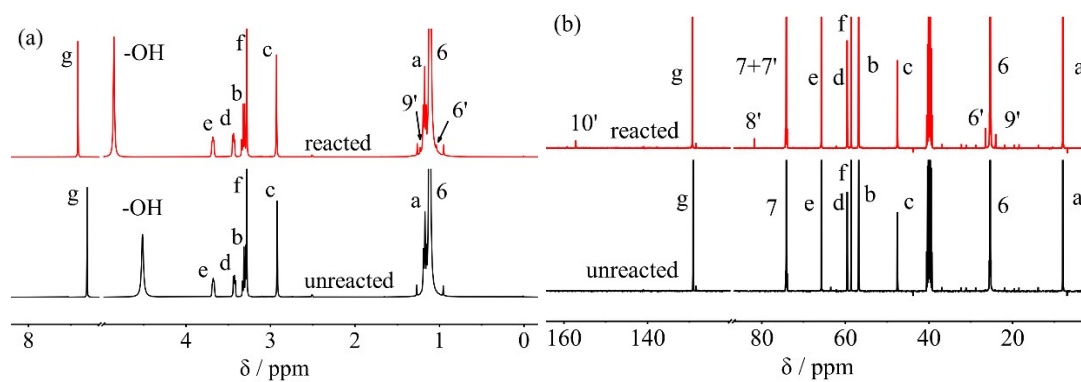
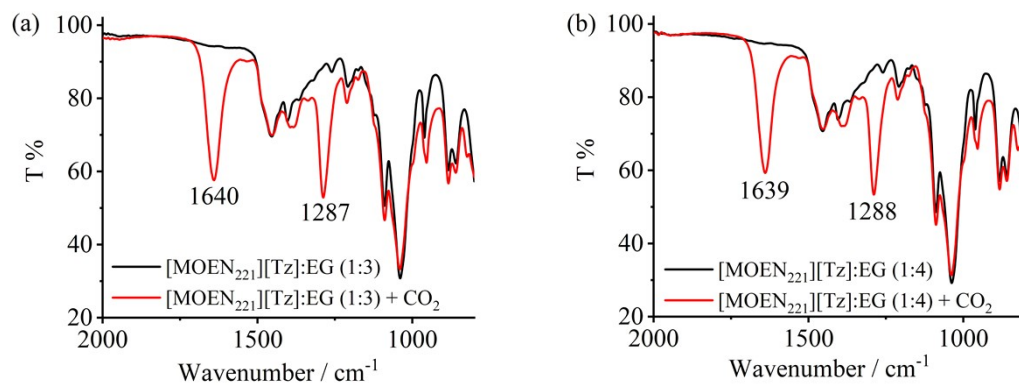**Fig. S5** The ^1H (a) and ^{13}C (b) NMR spectra of $[MOEN_{221}][Tz]$:PIN (1:4) before and after CO_2 uptake.

Fig.S6 FTIR spectra of $[MOEN_{221}][Tz]:EG$ (1:3) (a) and $[MOEN_{221}][Tz]:EG$ (1:4) (b) before and after CO_2 absorption.
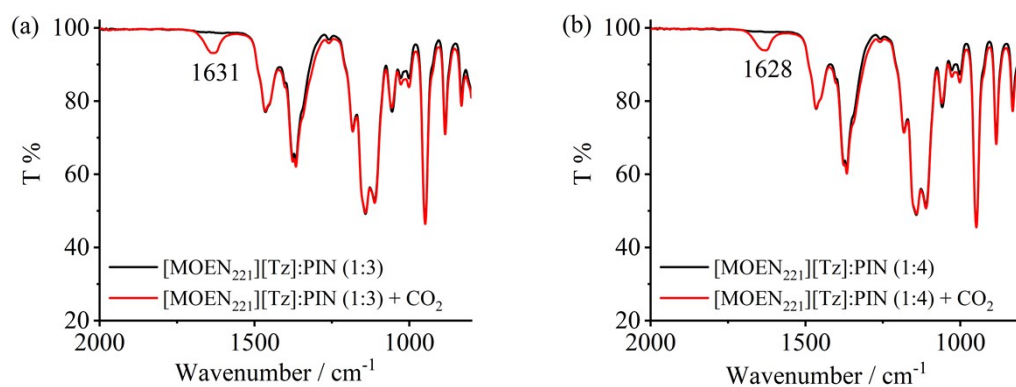

Fig.S7 FTIR spectra of $[MOEN_{221}][Tz]:PIN$ (1:3) (a) and $[MOEN_{221}][Tz]:PIN$ (1:4) (b) before and after CO_2 absorption.
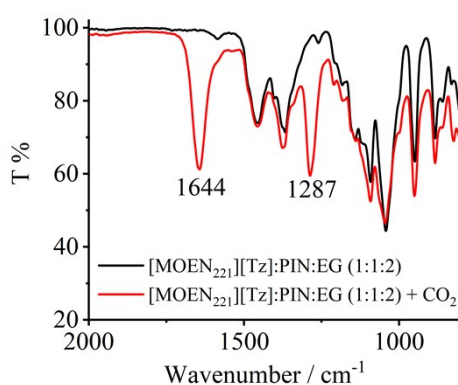
Fig.S8 FTIR spectra of $[MOEN_{221}][Tz]:PIN:EG$ (1:1:2) before and after CO_2 absorption.
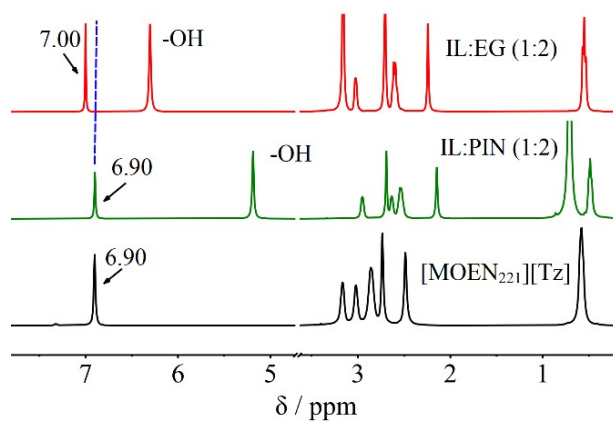
Fig. S9 The ^{1}H NMR spectra of [MOEN$_{221}$][Tz], [MOEN$_{221}$][Tz]:EG (1:2), and [MOEN$_{221}$][Tz]:PIN (1:2) in their neat state using DMSO-d$_{6}$ as the external solvent .
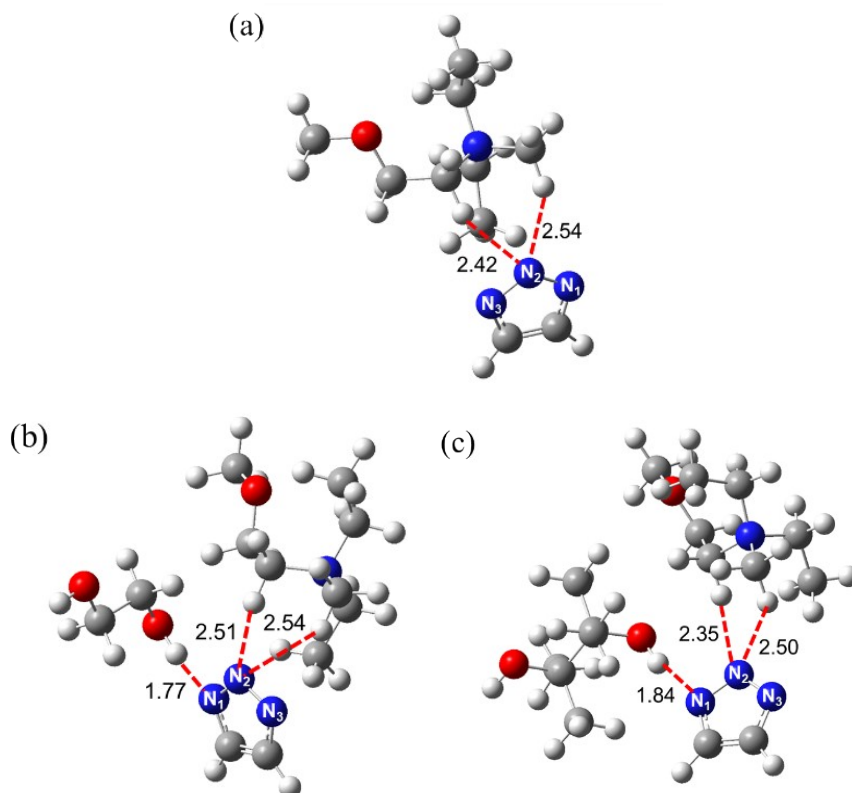
Fig. S10 The optimized structures of [MOEN$_{221}$][Tz] (a), [MOEN$_{221}$][Tz]–EG (b) and [MOEN$_{221}$][Tz]–PIN (c). Color code: gray – carbon; white – hydrogen; red – oxygen; blue – nitrogen. Dashed lines are hydrogen bonds.

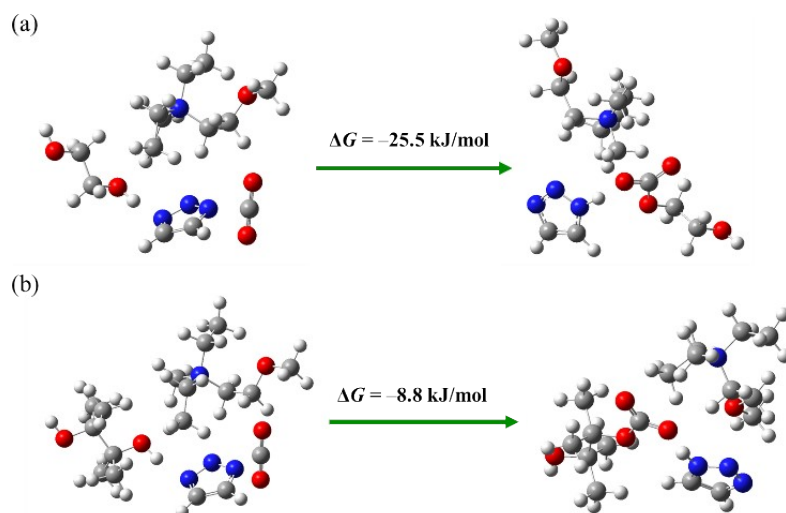**Fig. S11** The reactions of CO_2 with $[MOEN_{221}][Tz]$–EG (a) and $[MOEN_{221}][Tz]$–PIN (b). Color code: gray – carbon; white – hydrogen; red – oxygen; blue – nitrogen.
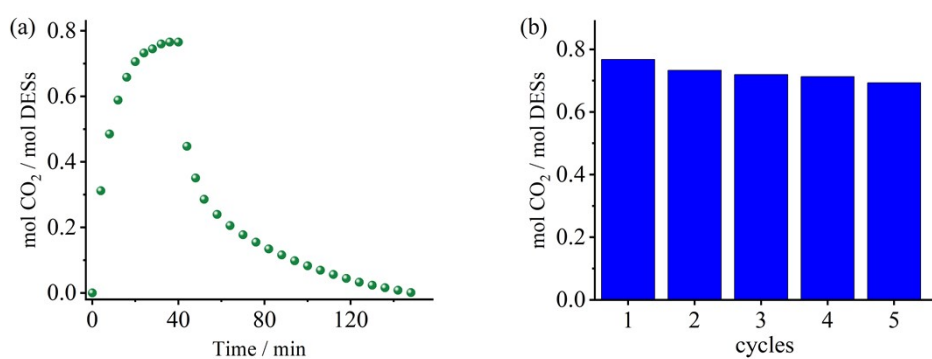

Fig. S12 (a) CO_2 absorption and desorption by $[MOEN_{221}][Tz]$:EG (1:2) (absorption:25°C, desorption: 35°C); (b) Five consecutive absorption and desorption cycles by $[MOEN_{221}][Tz]$:EG(1:2).

References

1   Z. Wang, M. Chen, B. Lu, S. Zhang, D. Yang, *ACS Sustainable Chem. Eng.* **2023**, *11*, 6272-6279.

2   M. Chen, Y. Zhou, Q. Lu, D. Yang, *Chem. Commun.* **2024**, *60*, 7061-7064.

3   M. J. Frisch, G. W. Trucks, H. B. Schlegel, G. E. Scuseria, M. A. Robb, J. R. Cheeseman, G. Scalmani, V. Barone, G. A. Petersson, H. Nakatsuji, X. Li, M. Caricato, A. V. Marenich, J. Bloino, B. G. Janesko, R. Gomperts, B. Mennucci, H. P. Hratchian, J. V. Ortiz, A. F. Izmaylov, J. L. Sonnenberg, D. Williams-Young, F. Ding, F. Lipparini, F. Egidi, J. Goings, B. Peng, A. Petrone, T. Henderson, D. Ranasinghe, V. G. Zakrzewski, J. Gao, N. Rega, G. Zheng, W. Liang, M. Hada, M. Ehara, K. Toyota, R. Fukuda, J. Hasegawa, M. Ishida, T. Nakajima, Y. Honda, O. Kitao, H. Nakai, T. Vreven, K. Throssell, J. A. Montgomery, Jr., J. E. Peralta, F. Ogliaro, M. J. Bearpark, J. J. Heyd, E. N. Brothers, K. N. Kudin, V. N. Staroverov, T. A. Keith, R. Kobayashi, J. Normand, K. Raghavachari, A. P. Rendell, J. C. Burant, S. S. Iyengar, J. Tomasi, M. Cossi, J. M. Millam, M. Klene, C. Adamo, R. Cammi, J. W. Ochterski, R. L. Martin, K. Morokuma, O. Farkas, J. B. Foresman, and D. J. Fox, Gaussian 16, Revision A.03, Gaussian, Inc., Wallingford CT, 2016.

4   Y. Zhao, D. G. Truhlar, *Theor. Chem. Acc.* **2008**, *120*, 215-241.

5   F. Weigend, R. Ahlrichs, *Phys Chem Chem Phys* **2005**, *7*, 3297-3305.

6   A. V. Marenich, C. J. Cramer, D. G. Truhlar, *J. Phys. Chem. B* **2009**, *113*, 6378-6396.